

Multi-Level Anomaly Detection on Streaming Graph Data

Robert A. Bridges*[†] John Collins[†] Erik Ferragut[†] Jason Laska[†] Blair D. Sullivan[‡]

Abstract

As a natural structure for representing entities and interactions, graphs are commonly used in many domains. Because of inherent complexity, converting graph data to meaningful information through analysis or visualization is often challenging. Identifying patterns and aberrations in graph data can pinpoint areas of interest, provide context for deeper understanding, and enable discovery in many applications.

This work presents a novel modeling and analysis framework for graph sequences. The framework addresses the issues of modeling, detecting anomalies at multiple scales, and enabling understanding of graph data. A new graph model, generalizing the BTER model of Seshadhri et al. by adding flexibility to community structure, is introduced and used to perform multi-scale graph anomaly detection. Specifically, probability models describing coarse subgraphs are built by aggregating probabilities at finer levels, and these closely related hierarchical models simultaneously detect deviations from expectation. This technique provides insight into the graph’s structure and internal context that may shed light on a detected event. Additionally, this multi-scale analysis facilitates intuitive visualizations by allowing users to narrow focus from an anomalous graph to particular subgraphs causing the anomaly. For evaluation, two hierarchical anomaly detectors are tested against a baseline on a series of sampled graphs. The superior hierarchical detector outperforms the baseline, and changes in community structure are accurately detected at the node, subgraph, and graph levels. To illustrate the accessibility of information made possible via this technique, a prototype visualization tool, informed by the multi-scale analysis is tested on NCAA football data. Teams and conferences exhibiting changes in membership are identified with greater than 92% precision and recall. Screenshots of an interactive visualization, allowing users to probe into selected communities, are given.

1 Introduction

As the scale and availability of scientific and engineering data grows, it has become increasingly important for analysts to understand the interactions among elements and detect changes over time. Often, it helps to represent the data as a set of graphs, where edges naturally encode relationships. The key question then becomes how to distinguish “normal” graphs/subgraphs/nodes from abnormal or anomalous ones and understand anomalies in context. For instance, in a cyber-security setting, observing an unanticipated connection (e.g., edge) between an internal IP and an external host may warrant alarm, yet furnished with the additional information that many similar IP’s (e.g., nodes in a common community) contact that host regularly may save an unnecessary investigation. Given a sequence of graphs (which can be thought of as corresponding to data collected over time), our work seeks to identify discrepancies from the baseline in a newly observed graph and present them in a context that facilitates understanding. To this end, we simultaneously track probability models and detect aberrations at the node, subgraph, and entire graph levels. This multi-scale approach allows end-users to quickly and easily focus their attention on the most critical changes in the data.

We give a novel method for multi-scale detection in time-varying graph data, using hierarchically related distributions to detect related anomalies at three increasingly fine levels of granularity. Further, we present an extension to a popular generative graph model that enables more accurate modeling of degree distribution and community structure; insights into the challenges of using graph models for anomaly detection, especially when node labels are kept; and a prototype of interactive visualization software that leverages the multi-scale analysis to enable users to easily explore the details of discovered anomalies in the data.

In order to perform probabilistic multi-scale detection, one needs an underlying graph model for comparison. In Section 3, we define our model – an extension of the recent BTER model that enables improved prescription of community structure. To fit an instance of the model to observed graphs, we give methods for detecting communities and estimating parameters in Section 4. Finally, to test a newly observed graph for anomalous

*Lead author. Email: bridgesra@ornl.gov.

[†]Oak Ridge National Laboratory

[‡]Dept. of Computer Science, North Carolina State University.

structure, we compute hierarchically-related probabilities from the tuned model and their associated p -values (which may require a Monte-Carlo simulation). Section 5 defines the probability calculations of two multi-scale detectors, as well as a baseline detector similar to that of [13]. While intuitive, performing anomaly detection using the graph’s probability—as given by the model from which it was sampled—will often result in an inaccurate detector when node labels are used. This is a consequence of the likelihood of an unlabeled graph being shared by isomorphic copies distinguished by these labels and is discussed in Section 6. We argue (and provide empirical evidence) that modeling a set of statistics indicative of node/subgraph interactions provides more accurate detection. In Section 7, we apply our detector to NCAA Football data, establishing its accuracy in detecting variations in teams’ schedules as imposed by changes in conference membership. Finally, we describe (and show sample screenshots of) our interactive anomaly visualization tool.

2 Related Work

Previous efforts in the literature for graph anomaly detection exist and can broadly be categorized as using compression techniques such as [4] or a form of hypothesis testing with graph statistics, e.g., [11, 12, 13]. Eberle & Holder use a compression algorithm relying on minimum description length to detect repetitive subgraphs and identify slight deviations as anomalies [4]. Because this technique searches for subgraphs almost isomorphic to a found normative pattern, it is a much more rigid detection framework than ours. In [11, 12] Miller et al. perform network anomaly detection using a hypothesis testing framework with various statistics all based on the residual matrix. Much of the work is geared towards detecting an R-MAT graph with abnormally dense communities artificially added. In [11] the techniques are extended to include methods for identifying unusually connected regions and can accommodate the streaming graph setting. While Miller et al.’s method for finding anomalous subgraphs are limited to identifying abnormally dense regions, our technique can find more general deviations including an influx, decrease, or simply unexpected interactions.

Recent work of Neville & Moreno also perform network hypothesis testing by fitting Gaussian distributions to three statistics [13]. Similar to our overall workflow, a p -value, estimated by a Monte-Carlo simulation from a graph model is used to decide anomalies, although no multi-scale detection is provided. Because of the similarity to [13], we test our method against a baseline detector similar to theirs. We note that because [13] focused on a different graph model the efficacy of

the statistics may vary, and, consequently, it is not a direct comparison. Details are in Section 6.

To the authors’ knowledge, using multiple related detectors that respect the structure of the graph is a new technique. By design, this analysis informs an interactive visualization allowing users to probe into detected graphs and explore the nature of abnormalities. While there is an extensive literature on graph visualization, relatively little explores the possibilities for interactive graph exploration. Wong et al. [17] present a multi-scale tool for exploring large graphs, informed by a clustering algorithm especially tuned to detecting star-burst patterns. In contrast, we have adopted a clustering approach that detects highly connected communities and married the multi-scale visual-analytics with anomaly detection.

2.1 Anomaly Detection Previous work by Feragut et al. [6] has developed and analyzed a general work-flow for anomaly detection that is extended to hierarchically analyze graph data in this work. The general method estimates probability models from observations and new data is declared anomalous if it has sufficiently small p -values. More precisely, if probability distribution, P , is estimated from observed data x_1, \dots, x_{n-1} , the p -value of new data, x_n , is

$$p\text{-value}(x_n) = P(\{X : P(X) \leq P(x_n)\}).$$

Notice that in the stereotypical case where $P = \mathcal{N}(0, 1)$, the standard normal, the definition above corresponds to the 2-sided p -value. Generally, a threshold $\alpha \in [0, 1]$ is set, and if $p\text{-value}(x_n) \leq \alpha$, x_n is identified as anomalous. The cycle then repeats as the model parameters are updated to include the new observation, x_n , so this is a streaming anomaly detection framework. Analysis in [6] identify operational benefits of the method including a theorem allowing users to regulate the expected alert rate *a priori*. In addition to the operational benefits, this framework’s accommodation of any probability model allows it to be used simultaneously at hierarchical levels.

2.2 Generative Graph Models Historically, the Erdős-Rényi generative model [5], denoted here as $ER(n, p)$, in which n nodes are fixed and edges occur independently with probability p , has received ample attention from the theoretical research community. More recently, as graphs are increasingly used to represent a myriad of data sources, a trend to discover cross-cutting themes in the graph data and build models that can accurately capture those themes has produced many random graph models. For example, the Chung-Lu (CL) model [3] and Barabàsi-Albert preferential attachment

model [1] can accommodate expected scale-free degree distributions. A survey of graph models and common graph patterns is given in [2].

For this work, a generative model that can accommodate observed hierarchical structure is needed, and we focus on community structure. Stochastic Block models, first introduced in [9], allow assignment of communities, but the expected degree of each node is dependent on its community's size and interaction with other communities. Very recently, the Block Two-Level Erdős-Rényi (BTER) model [10, 15] uses an implicit community structure to model degree distribution along with clustering coefficient especially of small degree nodes. The main drawback of BTER (from our perspective) is the rigidity of community membership, size, and edge densities; thus, a new model, which allows more flexible modeling of communities, is introduced (Section 3).

3 The Generalized BTER Model (GBTER)

In order to perform probabilistic anomaly detection, we need a randomized generative graph model that enables computation of probabilities for various graph configurations, while accurately modeling a graph's community structure and degree sequence. Significant prior work has been devoted to developing such models and validating the importance of capturing both these aspects of a real-world data set (e.g., [1, 2, 3, 10, 15]). A natural candidate is a Stochastic Block Model, which defines community membership and generates intra-community edges with an ER model and inter-community edges with a probability that depends on the membership of their endpoints. This achieves flexible community membership and density, but the expected degree of each node is implicitly determined by the community structure and parameters. To improve adherence to degree distribution, one could use the Block Two-Level Erdős-Rényi (BTER) of Seshadhri et al. [15], but we find the implicitly determined community structure of the model to be too limiting for matching real-world data. BTER edge generation occurs in two steps, with an Erdős-Rényi (ER) model used for intra-community edges followed by a Chung-Lu (CL) process to match a specified expected degree distribution. Thus, to obtain a model for our needs, we define and use a generalization of BTER that mimics its two-step edge generation process, but allows explicit prescription of the communities' size, membership, and approximate density. The remainder of this section describes this generalized version, and compares it to the original BTER model.

The generalized block two-level Erdős-Rényi (GBTER) model takes as input (1) the expected degree of each node i , (2) community assignments of the

nodes, i.e., a partition of the vertex set into disjoint subsets, $\{C_j\}$, and (3) an edge probability p_j for each community C_j . In the first stage of edge generation, intra-community edges are sampled from an ER random graph model, $\text{ER}(|C_j|, p_j)$ for each community C_j . Note the expected degree of a node in C_j is $p_j(|C_j| - 1)$ after the first stage. In the second stage, we define the *excess expected degree* of a node i , denoted ε_i , to be the difference between the input expected degree λ_i and the expected degree after stage one. Formally, $\varepsilon_i := \max(0, \lambda_i - p_j(|C_j| - 1))$ for node i in community C_j . We then apply a Chung-Lu style model [3] on the *excess expected degree*-sequence, $[\varepsilon_i]_{i \in V}$. Specifically, the probability of adding the edge (i, j) , is

$$(3.1) \quad P(i, j | \varepsilon) = \frac{\varepsilon_i \varepsilon_j}{\sum_k \varepsilon_k}.$$

Note that the second stage can generate both inter- and intra-community edges. It is necessary that Chung-Lu inputs, $\{\varepsilon_i\}$, satisfy $\varepsilon_i \varepsilon_j \leq \sum_k \varepsilon_k$ for Equation 3.1 to define a probability. A calculation shows that the expected degree of node i is indeed d_i whenever $d_i \geq p_j(|C_j| - 1)$ (i.e., the expected degree from the first-stage edges does not exceed the total expected degree of any node), and the CL model is well-defined.

To calculate the probability of edge (i, j) , we condition on whether i and j share a community. If i, j are both assigned to community C , let p denote the internal edge probability of C , and we see

$$(3.2) \quad P(i, j | i, j \in C) = p + (1 - p) \frac{\varepsilon_i \varepsilon_j}{\sum_k \varepsilon_k}.$$

If i, j are assigned to different communities, the edge probability is as given in Equation 3.1.

GBTER differs from the original BTER model by allowing greater flexibility and assignment of community membership, size, and internal edge density (p). As indicated in [10], the expected clustering coefficient for an $\text{ER}(n, p)$ graph is p^3 . This implies that GBTER also allows pre-specification of each community's approximate clustering coefficient. Note that GBTER, as used in this work, assumes node labels, but BTER on the other hand only depends on the number of nodes of each expected degree. This implies that edges in BTER do not occur independently (because they are conditioned on the community assignment of each node), while they are independent in GBTER. Consequently, calculating probabilities of graphs according to the BTER model is both complicated and expensive, inhibiting its use for anomaly detection.

4 Fitting Model Parameters

We now describe how to fit the GBTER model to a sequence of observed graphs with common node labels us-

Table 1: Community assignments for GBTER Experiment

	C_1	C_2	C_3	C_4	...	C_{10}
M_r	[0,1,2,3]	[4,5,6,7]	[8,9,10,11]	[12,13,14,15]	...	[36,37,38,39]
M_a	[0, 11 , 2, 4]	[3 , 5, 6, 8]	[7 , 9, 10, 1]	[12,13,14,15]	...	[36,37,38,39]

Note: The seeded-anomaly model M_a is obtained from M_r by switching the position of 2 nodes from each of the first 3 communities. Anomalous nodes and shown in italicized red, and anomalous communities are circled.

ing Bayesian techniques for learning the parameters and inferring the following model inputs: (1) the community assignments, (2) the within-community edge densities, and (3) the expected node degrees. Once a specific instance of the model is deduced, probabilistic anomaly detectors are constructed, as detailed in Section 5.

In this work, a partition of the vertex set into communities is learned using the Markov Clustering (MC) algorithm [16]. A description of the MC algorithm is included in the supplemental material. To apply MC, a weighted graph is constructed by counting the occurrence of each edge in observations. For the experiments in Section 6, the weighted graph is constructed by counting the occurrence of each edge, and for the application in Section 7 exponential weights are used to down-weight older observation of edges. In general, any method of partitioning nodes into communities acceptable for the application at hand will suffice. For a survey of community detection algorithms see [7]. This work uses a data-driven approach. However, communities inferred from context (e.g., grouping nodes by a known, common affiliation) can be used to obviate this step and may provide more insightful results in a real-world setting.

Given community assignments, the within-community edge densities are estimated. Each community, C , is modeled internally by an Erdős-Rényi random graph, $\text{ER}(|C|, p)$, and we seek to estimate p . Letting k denote the number of edges within the subgraph C , it follows that $k \sim \text{Binomial}(\binom{|C|}{2}, p)$. In order to use Bayesian inference, we assume $p \sim \text{Beta}(\alpha, \beta)$.

Hence,

$$(p|k_1, \dots, k_N) \sim \text{Beta}(\alpha + \sum_i k_i, \beta + N \binom{|C|}{2} - \sum_i k_i),$$

where k_i denotes the number of edges internal to C observed in the i -th graph, G_i , for $i = 1, 2, 3, \dots, N$. Altogether, to generate p , we sample p from this posterior Beta with prior parameters $\alpha = \beta = 1$.

Lastly, the expected degree sequence must be estimated from the data. For a fixed node, we assume its degree, d , is Poisson distributed with expected degree λ , i.e. $d \sim \text{Poisson}(\lambda)$. We use the conjugate prior,

$\lambda \sim \text{Gamma}(\alpha, \beta)$, which yields

$$(\lambda|d_1, \dots, d_N) \sim \text{Gamma}(\alpha + \sum_i d_i, \beta + N)$$

where d_i denotes the observed degree of the node in G_i . For each node, we generate its expected degree, λ , by sampling from the posterior Gamma with prior parameters $\alpha = \beta = 2$.

5 Multi-Scale Anomaly Detectors

Given an instance of a GBTER model, the probabilistic description can be used to detect anomalies at the graph, subgraph, and node level. This section defines two multi-scale detectors. The Graph Probability Detector, intuitively uses the graph probability, as determined by the GBTER model, for detection, which is then decomposed into probabilities of subgraphs for hierarchical information. A second detector, the Graph Statistics Detector, builds from the bottom up, defining the probability of a node based on the likelihood of its internal and external degree. Subgraph probabilities are determined by those of its member nodes. Lastly, a baseline method for detecting anomalous graphs by fitting Gaussian distributions to graph statistics, is described. The subsequent section, 6, gives results of testing the three methods on manufactured data.

5.1 Graph Probability Anomaly Detector This first anomaly detector uses the graph probability, as given by the GBTER model, for anomaly detection. Specifically, given a graph $G = (V, E)$ with vertices V and edges E , the probability of G is

$$(5.3) \quad P(G) = \prod_{(i,j) \in E} P(i,j) \prod_{(i,j) \notin E} (1 - P(i,j)),$$

where $P(i,j)$ is the probability of the edge (i,j) under the GBTER model. See Section 3 for a derivation of $P(i,j)$. In practice, given a graph G , we compute its probability using Equation 5.3, then use Monte-Carlo simulation to estimate its p -value.

In order to detect anomalies at different scales, the probability of a graph, as given above, is decomposed into a product of subgraph probabilities. Specifically,

we define the probability of node i_0 as

$$P(i_0) := \prod_{j:(i_0,j) \in E} P(i_0, j) \prod_{j:(i_0,j) \notin E} (1 - P(i_0, j)).$$

It follows that $P(G) = \prod_i P(i)^{1/2}$. Similarly, the probability of a subgraph $G' = (V', E')$ is $\prod_i P(i)^{1/2}$, with the product over $i \in V'$. Hence, given a partition of V into communities, $\{C_i\}$, the probability of G also breaks into a product of community probabilities, i.e., $P(G) = \prod_i P(C_i)$. This formulation allows anomaly detection of any fixed subgraph, in particular at the node, community, and graph level.

5.2 Graph Statistics Anomaly Detector In addition to the method above, a detection method based on graph statistics is also tested. After learning the GBTER parameters, the intra- and inter-community degrees of each node are observed and modeled to provide a basis for this detector.

Fix a node $i_0 \in V$, and let C denote i_0 's community, p denote C 's intra-community edge probability, and λ the expected degree of node i_0 (all as learned from fitting the GBTER model to our observations). We set $d_{in} := |\{(i_0, j) \in E : j \in C\}| = i_0$'s internal degree, and $d_{ex} := |\{(i_0, j) \in E : j \notin C\}| = i_0$'s external degree. Following the $ER(|C|, p)$ assumption, we assume $d_{in} \sim \text{Binomial}(|C| - 1, p)$, and $d_{ex} \sim \text{Poisson}(\varepsilon)$, where $\varepsilon = \max(0, \lambda - p(|C| - 1))$, is the excess expected degree of i_0 (see Section 3). For the graph statistics anomaly detector, the probability of node i_0 is defined as the joint probability of its degrees. We assume the two degrees are independent and obtain,

$$P(i_0) := P(d_{in}, d_{ex}) = \binom{|C| - 1}{d_{in}} p^{d_{in}} (1 - p)^{|C| - 1 - d_{in}} \frac{e^{-\varepsilon} \varepsilon^{d_{ex}}}{d_{ex}!}$$

Given a subgraph $G' = (V', E')$ we set $P(G') := \prod_{V'} P(i)$. Hence anomaly detection of any subgraph is made possible.

Note that since GBTER allows both internal and external edges to be created by the second stage of the process, the model above inflates internal degree d_{in} and deflates d_{ex} compared to GBTER. Additionally, as the range of a Poisson variable is unbounded, degrees exceeding $|V| - 1$ (an impossibility) are assigned positive probability by this model. To circumvent this possibility, the truncated Poisson can be used for sampling. In our experiments, the expected degree (λ) and expected excess degree (ε) are sufficiently smaller than $|V| - 1$, which implies the $P(\deg(i) > |V| - 1)$ is negligible. Testing with and without the truncation exhibited similar results.

5.3 Gaussian Baseline Detector The two detectors described above are tested against a baseline method that fits univariate Gaussian distributions to graph statistics and uses the product of the p -values for detection. From each observed graph three statistics are obtained: average node degree (X_1), average clustering coefficient (X_2), and the spectral norm (X_3). Calculating X_1 and X_2 from a given graph is straightforward. In order to calculate X_3 , the GBTER model is used with parameters estimated as described above. After computation of the observed statistics, independent univariate Gaussian distributions ($\mathcal{N}(\mu_i, \sigma_i)$) are fit to each of the three statistics. Lastly, given a newly observed graph, G , with statistics $x_i, i = 1, 2, 3$, we assign

$$p\text{-value}(G) := \prod_{i=1}^3 P(X_i \leq x_i | \mathcal{N}(\mu_i, \sigma_i)).$$

As before, p -values falling below a given threshold, α , are labeled anomalous, and the three normal distributions are updated upon receipt of each new graph.

This baseline detector follows that of Moreno and Neville [13] where it is used on Mixed Kronecker Product graphs, although their work uses average geodesic distance instead of the spectral norm we employ for X_3 . Between the null-hypothesis and anomalous models used in our experiment we expect similar average geodesic; hence, this statistic is not discriminatory in our setting. The spectral norm statistic chosen instead has been used previously for network hypothesis testing and exhibited strong results for similar tests involving Chung-Lu random graphs [12]. While we consider this baseline a natural adaptation of [13], the disparity in graph models between their and our application inhibits direct comparison.

6 Synthetic Graph Experiment

In order to test the anomaly detection capabilities, two hidden GBTER models are used to generate labeled data, (1) a “regular” model, M_r , for sampling non-anomalous graphs, and (2) a seeded-anomaly model, M_a , with slightly perturbed inputs to generate anomalous graph. To begin the experiment, 100 non-anomalous graphs are sampled from M_r , and the anomaly detectors are fit to the data, as described in Section 5. To test the streaming anomaly detection, 500 graphs are iteratively generated and observed from with every fifth graph from the seeded anomaly model. Upon sampling a new graph, its p -value according to each anomaly detector is computed, and it is labeled as anomalous if it falls below a given threshold. Similarly, the hierarchical detectors label each node and community depending on its respective p -value. Lastly, each

Figure 1: Synthetic Data Experiment ROC Curves, Graph Level (Left), Community Level (Center), Node Level (Right), Experiment 1 (Top Row), Experiment 2 (Bottom Row)

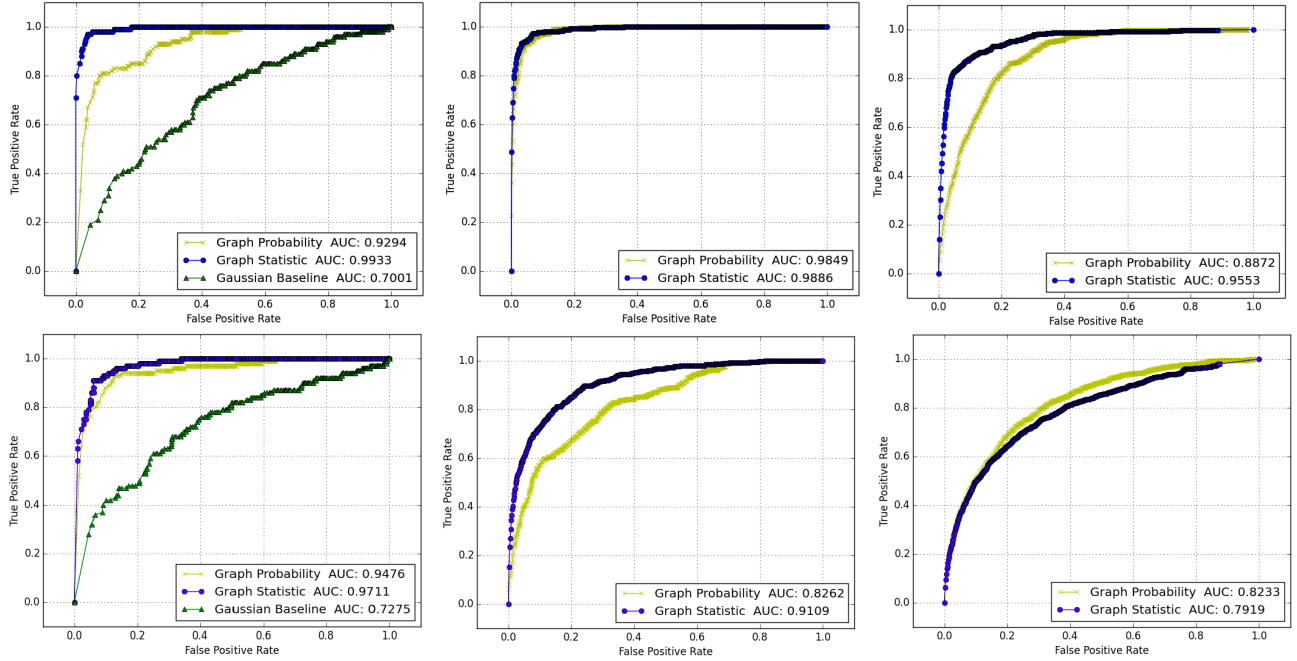


Table 2: GBTER Experiment Results (α maximizing F1)

Method	α	F1	P	R
Experiment 1				
Graph Level				
Graph Probability	0.010	0.766	0.762	0.770
Graph Statistic	0.014	0.915	0.866	0.970
Gaussian Baseline	0.052	0.434	0.313	0.710
Community Level				
Graph Probability	0.011	0.772	0.784	0.760
Graph Statistic	0.006	0.824	0.828	0.820
Node Level				
Graph Probability	0.018	0.273	0.223	0.353
Graph Statistic	0.011	0.556	0.495	0.633
Experiment 2				
Graph Level				
Graph Probability	0.004	0.792	0.826	0.760
Graph Statistic	0.020	0.847	0.791	0.910
Gaussian Baseline	0.028	0.467	0.379	0.610
Community Level				
Graph Probability	0.071	0.433	0.373	0.515
Graph Statistic	0.017	0.570	0.619	0.528
Node Level				
Graph Probability	0.026	0.350	0.332	0.370
Graph Statistic	0.034	0.340	0.327	0.355

anomaly detector’s model is updated to include observation of the new graph.

We conduct 2 experiments. Across both the “regular” and seeded-anomaly model, 40 nodes are divided into 10 communities of size 4. For the “regular” model, each community is assigned a within-edge probability of $p = .8$, and the expected degrees of nodes vary in the range of 5 to 8 according to a truncated power-law. To create the seeded-anomaly model for the first experiment, 2 nodes from each of the first 3 communities are interchanged resulting in 6 (of 40) anomalous nodes and 3 (of 10) anomalous communities per anomalous graph (see Table 1). For the second experiment, community assignments are held constant, but the within-community density (p) of the first 4 communities is changed from $.8$ to $.4$ in the seeded-anomaly model, and the expected degree of the nodes in these 4 communities is increased by 2. This will decrease intra-community, and increase extra-community interaction for these 4 communities. All together the second experiment has 4 (of 10) anomalous communities, and 16 (of 40) anomalous nodes per anomalous graph. To evaluate the detectors’ performance, the Receiver Operator Characteristic (ROC) curve, and area under the ROC curve (AUC) are displayed in Figure 1. Table 2 includes Precision, Recall, and F1 for each detector at the threshold α maximizing its F1 score. The Graph Statistic Model outperforms the other two models in all

cases except Experiment 2 node level detection.

The Graph Probability Model, which uses the probability of sampling a graph under a given generative model, is an intuitive choice for anomaly detection. Upon further examination, this technique yields poor results in models where the mode of the distribution varies depending on whether labels are regarded. As an illustrative example, consider the ER model on three labeled nodes, $V = \{1, 2, 3\}$ with $p = 1/3$. The most probable unlabeled graph under this distribution has exactly one edge, and occurs with probability $\binom{3}{1}(1/3)(2/3)^2 = 4/9$. Now labeling nodes, there are three different but isomorphic graphs with one edge each, namely, with edge $(1, 2)$ or $(2, 3)$ or $(1, 3)$ only. But the probability of each of these one-edge graphs is $(1/3)(2/3)^2 = 4/27$, while the probability of the empty graph is $(2/3)^3 = 8/27$. Hence when labels are regarded, the mode of the distribution is the empty graph, not the one-edge graphs as in the unlabeled case; consequently, in this case the Graph Probability Model will view the expected graphs as more anomalous than the less likely empty graph! Now consider the GBTER model used in the experiment above. Because the probability of an within-community edge is greater than .5 and inter-community edge is less than .5 with the given parameters, the labeled mode of the distribution is the graph with every community as a clique and no other edges. Although this graph is unlikely to be sampled, the Graph Probability Model will regard it as the most “normal” possible graph. The conclusion of this analysis is that using the graph’s probability will result in inaccurate detectors, and this is exhibited in our empirical results.

7 NCAA Football Data Experiment

To illustrate the insight given by multi-scale anomaly data, the Graph Statistics Model is used on NCAA Football data¹. Each season is represented as a graph with a node for each Division I team and an edge for each game played. Seasons 2008-2010 are used to train the GBTER model, and the streaming detection is performed on years 2011 and 2012. That is, after detecting anomalous communities and nodes in year 2011, the GBTER parameters are updated to include the 2011 season and applied to 2012. This data set was chosen for two reasons, (1) NCAA conferences give a ground truth community structure to the graph, and (2) conference membership was relatively constant in the 2008-2010 seasons and, experienced changes in 2011 and 2012. The GBTER parameters are learned as discussed in Section 5. Communities are detected using Markov clustering as before but with exponential down-weighting of previous

years’ edges as in Section 3. With appropriate configuration of Markov clustering parameters, the communities identified match almost identically with actual conferences, and we à posteriori label/refer to communities by the corresponding conference name.

Table 4: 2011 & 2012 most anomalous conferences displayed with p -value and number of membership changes.

2011	p -value	n	2012	p -value	n
MWC	0.000	3	WAC	0.000	5
PAC-10	0.000	2	Big-12	0.000	4
Big-12	0.000	2	MWC	0.000	4
Big-10	0.000	1	Big-East	0.000	2
WAC	0.000	1	SEC	0.000	2
CUSA	0.000	0	MAC	0.000	2
ACC	0.001	0	Sun-Belt	0.000	1
SEC	0.258	0	PAC-10	0.013	0
Sun-Belt	0.375	0	CUSA	0.206	0
MAC	0.654	0	ACC	0.983	0
Big-East	0.864	0	Big-10	0.988	0

7.1 Football Data Results Table 4 ranks the most anomalous conferences detected each year. Each conference experiencing a change in membership are detected is maximally anomalous, with p -value = 0. Recall that after computing the communities’ probability, their p -value is ascertained by a Monte-Carlo simulation; thus, p -value = 0 indicates all 1000 graphs sampled in the simulation exhibit higher probability. The 2011 community results produce one false positive, as CUSA is given an equivalently small p -value. At the conference level this gives perfect precision, and $12/13 = .92$ recall.

Table 3 details the ten most anomalous teams from each season in decreasing order along with their p -value and ground truth conference memberships for the previous and current season. In 2011 Boise St., Utah, Colorado, BYU, and Nebraska are the teams which switched membership, and ranked, respectively, 1,2,3,4, and 6 most anomalous by the detector. Note that Washington St., Washington, and Arizona St., filling the 5,7, and 8 spots, are members of the PAC-10 which admitted two new teams in 2011. So while these three teams did not change conferences, their schedules changed substantially, now playing both Colorado and Utah instead of previous PAC-10 members. Examining 2012’s team results, we see exactly eight teams switched conferences and are identified at the top of the list.

¹<http://www.sports-reference.com/cfb/> with permission

Table 3: 2011 & 2012 Ten Most Anomalous Teams

Team	<i>p</i> -value	2010 Conf.	2011 Conf.	Team	<i>p</i> -value	2011 Conf.	2012 Conf.
Boise St.	2.339e-19	WAC	MWC	West Virginia	6.792e-12	Big-East	Big-12
Utah	4.389e-10	MWC	PAC-10	Missouri	1.179e-11	Big-12	SEC
Colorado	5.362 e-09	Big-12	PAC-10	Texas Christian	8.418e-11	MWC	Big-12
BYU	6.233e-08	MWC	-	Temple	1.092e-09	MAC	Big-East
Washington St.	7.649e-08	PAC-10	PAC-10	Texas A&M	6.756e-09	Big-12	SEC
Nebraska	8.131e-08	Big-12	Big-10	Nevada	3.309e-08	WAC	MWC
Washington	8.891 e-07	PAC-10	PAC-10	Fresno St.	3.897e-08	WAC	MWC
Arizona St.	1.613e-06	PAC-10	PAC-10	Hawaii	3.459e-06	WAC	MWC
San Jose St.	4.639e-06	WAC	WAC	Louisiana Tech	1.039e-04	WAC	WAC
Utah St.	4.717e-06	WAC	WAC	Louisiana-Mon.	1.194e-04	Sun Belt	SunBelt

Using threshold of $\alpha = 1e - 08$ detects all but one team that switched conferences with only one false positive, giving both precision and recall of $12/13 = .92$.

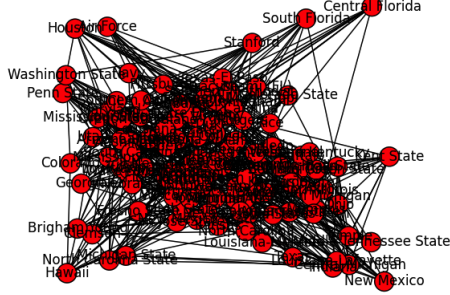
7.2 Interactive Data Visualization By design, the multi-scale analysis facilitates an interactive visualization tool allowing users to focus on and drill into noteworthy pieces of the graph. To illustrate the benefits, screenshots of a prototype visualization of the 2011 season’s data are given in Figure 2. While the 2011 graph, Figure 2.a, consists of only ~ 130 nodes with a well-defined community structure, an unprocessed visualization provides little insight into the anomalous sections of the graph. Alternatively, coarsening and displaying only “super”-nodes representing communities is a common technique for making the graph visualization informative and manageable. As informed by the community-level anomaly detectors, we display the community “super”-nodes colored so darker shades indicate more anomalous communities. In addition, the conference names and *p*-values are automatically applied so contextual information from the analysis and the domain are easily absorbed by a user. From Figure 2.b, an operator can quickly see the communities of interest and focus attention on the most anomalous areas of the graph. Our preliminary visualization includes clickable conference nodes that upon selection will display the conference subgraph with only its internal edges, again with nodes shaded to indicate anomalousness of the teams they represent. This setup facilitates drilling into the graph to discover anomalies, and the context in which they occur. For example, clicking on the MWC conference displays its image, Figure 2.c, from which it is immediately apparent that, while Utah and Brigham Young were previously members of that community, they cease to participate in the MWC. Similarly, the PAC-10 conference subgraph, Figure 2.d, exhibits strong density but each node is very anomalous,

indicating that the interaction outside the conference has changed.

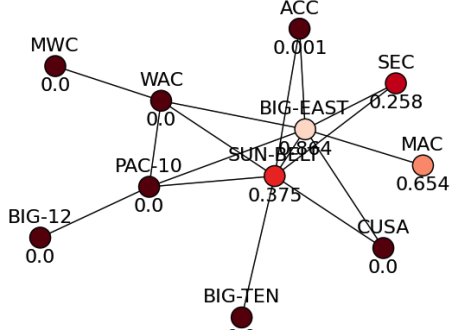
Altogether, the framework for multi-scale detection yields analytic results that are readily input into an interactive visualization. Upon detection of an anomalous graph, users can now zoom into areas of interest, and form and resolve hypotheses about how the anomaly occurred.

8 Conclusion

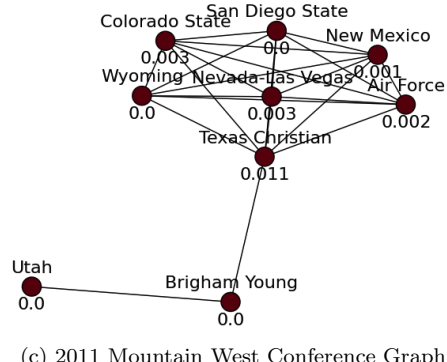
Our primary hypothesis—that detecting multiple related anomalies at different levels of granularity can facilitate deep insights into the nature of abnormalities—is examined in this work on both synthetic graph data and NCAA football data. This experimentation suggests that appropriate modeling of graph statistics yields more accurate detectors of anomalous graphs than by using a graph’s probability as given by a generative model, in particular when node labels are regarded. Additionally, our hierarchical Graph Statistics Detector has outperformed a previous detection method that fits Gaussian distributions to observed graph statistics when detecting changes in community structure. In both the synthetic experiment and the application to NCAA data, the Graph Statistics Detector’s ability to accurately pinpoint anomalies at the node, subgraph, and graph level are exhibited. We argue that the operational advantages of this technique—that users can focus time and effort on anomalies at various scales and, thereby, easily discover/examine the context with which an anomaly occurs—are established, as exemplified in the application to NCAA data. We believe this method is well-suited to aid operators in analyzing time-series data; hence, in future work we plan to apply this multi-scale visual-analytic technique to real-world data, such as, cyber, energy grid, or social network data. Additionally, as the GBTER model is only introduced in this work, a more thorough investigation of its model-



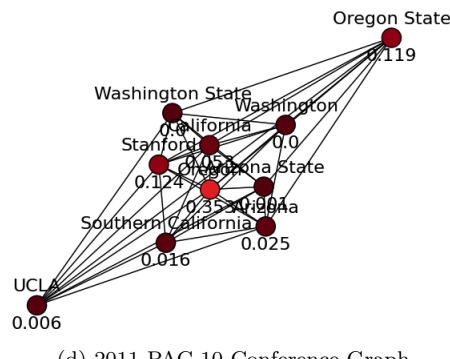
(a) Unprocessed 2011 Season Graph



(b) Coarsened 2011 Season Graph



(c) 2011 Mountain West Conference Graph



(d) 2011 PAC-10 Conference Graph

Figure 2: 2011 Season Graph interactive visualizations screenshots produced by Matplotlib using NetworkX [8] spring force directed layout. Team/conference labels applied in post-analysis along with p -values in (b)-(d). Darker colors correspond to more anomalous nodes.

ing abilities and applications to data sets is warranted.

9 Acknowledgements

This manuscript has been authored by a contractor of the U.S. Government under contract DE-AC05-00OR22725. Accordingly, the U.S. Government retains a nonexclusive, royalty-free license to publish or reproduce the published form of this contribution, or allow others to do so, for U.S. Government purposes.

B. Sullivan supported in part by the National Consortium for Data Science Faculty Fellows Program and the Defense Advanced Research Projects Agency under SPAWAR Systems Center, Pacific Grant N66001-14-1-4063. Any opinions, findings, and conclusions or recommendations expressed in this publication are those of the author(s) and do not necessarily reflect the views of DARPA, SSC Pacific, or the NCDS.

10 Appendix

This supplement provides the algorithm used for the streaming anomaly detection experiment and definitions from the graph theory literature used in our paper without explanation.

10.1 Clustering Coefficients Given a graph, $G = (V, E)$, the *global clustering coefficient*, denoted c , is defined as the ratio of the number of wedges incident to any node by the number of triangles incident to any node. Explicitly, if $T_j := |\{(i, j), (j, k), \text{ and } (k, i) \in E\}|$ is the number of triangles incident to node j , and $W_j := |\{(i, j) \text{ and } (j, k) \in E\}|$ is the number of wedges incident to j ,

$$(10.4) \quad c := \frac{\sum_{j \in V} T_j}{\sum_{j \in V} W_j}.$$

This definition can be restricted to subgraphs by changing the summation. As used in the BTER model, for a fixed degree, d , the clustering coefficient of nodes with degree d , denoted c_d is defined as in Equation 10.4 with summation only over those nodes with degree d . Lastly, as used in [13] and the Gaussian Baseline method described in subsection ??, *average clustering coefficient* is defined as the average of the clustering coefficient of each node; formally,

$$(10.5) \quad \frac{1}{|V|} \sum_{j \in V} \frac{T_j}{W_j}.$$

10.2 Spectral Norms Given both a graph and a generative graph model, the *spectral norm* is defined as the spectral radius of residual matrix, that is, the largest eigenvalue in absolute value. The residual matrix is

$A - E$, were A denotes the adjacency matrix of the given graph, and E is the expected adjacency matrix. The expected adjacency matrix entries are given by the edge probabilities, i.e., $E(i, j) := P(i, j)$, as determined by the graph model. This definition follows the formulation in [12].

Algorithm 1: Streaming Detection Experiment

Input: N = number of training graphs K = number of streamed graphs k = factor of streamed graphs to come from seeded anomaly model M_r = “regular” model M_a = seeded-anomaly model α = threshold

Output: $\{(G_{n_i}, p - \text{value}(G_{n_i}))\}$ = set of anomalous graphs with corresponding p -values

Initialize $Graphs \leftarrow \{\}$, $Anomalous \leftarrow \{\}$, $i \leftarrow 0$

while $i < N$ **do**

- | Sample G_i from M_r
- | Store G_i in $Graphs$
- | $i += 1$

Learn M_N (anomaly detector model) parameters from $Graphs$

while $i < N + K$ **do**

- | **if** $i \% k == 0$ **then**
- | | Sample G_i from M_a
- | **else**
- | | Sample G_i from M_r

 | Store G_i in $Graphs$

 | Set $pv \leftarrow P(\{G : P(G) \leq P(G_i)\} | M_{i-1})$

 | **if** $pv \leq \alpha$ **then**

- | | Store (G_i, pv) in $Anomalous$

 | Update M_i to M_{i+1} using $Graphs$

 | $i += 1$

return $Anomalous$

10.3 Geodesic Distances The *geodesic distance* between two nodes, i, j of a graph $G = (V, E)$ is the length of a shortest path between i and j , given such a path exists. In the case that i, j lie in different components, their geodesic distance is ∞ . Intuitively, the *average geodesic distance* of a graph G is the average of the geodesic distances over all possible pairs of nodes.

10.4 Markov Clustering Algorithm A brief description of the Markov Clustering Algorithm is provided below. The original citation is [16] and for completeness see [14]. The identity matrix is added to the graph’s adjacency matrix. Next this resultant matrix is converted to a row stochastic matrix, and the following five steps are iterated until convergence. First, the matrix is squared. Second, each element in the matrix is squared. Third, the matrix is row stochasticized. Fourth, entries with values below a given parameter are removed to save memory. Fifth the matrix is row stochasticized. However we have chosen parameter values such that the Fourth step is never completed since the graphs in this paper can fit into memory easily.

References

- [1] Albert-László Barabási and Réka Albert. Emergence of scaling in random networks. *science*, 286(5439):509–512, 1999.
- [2] Deepayan Chakrabarti and Christos Faloutsos. Graph mining: Laws, generators, and algorithms. *ACM Computing Surveys (CSUR)*, 38(1):2, 2006.
- [3] Fan Chung and Linyuan Lu. The average distances in random graphs with given expected degrees. *Proceedings of the National Academy of Sciences*, 99(25):15879–15882, 2002.
- [4] William Eberle and Lawrence Holder. Anomaly detection in data represented as graphs. *Intelligent Data Analysis*, 11(6):663–689, 2007.
- [5] Paul Erdős and Alfréd Rényi. On random graphs. *Publicationes Mathematicae Debrecen*, 6:290–297, 1959.
- [6] Erik M Ferragut, Jason Laska, and Robert A Bridges. A new, principled approach to anomaly detection. In *Machine Learning and Applications (ICMLA), 2012 11th International Conference on*, volume 2, pages 210–215. IEEE, 2012.
- [7] Santo Fortunato. Community detection in graphs. *Physics Reports*, 486(3):75–174, 2010.

- [8] Aric A. Hagberg, Daniel A. Schult, and Pieter J. Swart. Exploring network structure, dynamics, and function using NetworkX. In *Proceedings of the 7th Python in Science Conference (SciPy2008)*, pages 11–15, Pasadena, CA USA, August 2008.
- [9] Paul W Holland, Kathryn Blackmond Laskey, and Samuel Leinhardt. Stochastic blockmodels: First steps. *Social networks*, 5(2):109–137, 1983.
- [10] Tamara G Kolda, Ali Pinar, Todd Plantenga, and C Seshadhri. A scalable generative graph model with community structure. *arXiv preprint arXiv:1302.6636*, 2013.
- [11] Benjamin A Miller, Nadya T Bliss, Patrick J Wolfe, and Michelle S Beard. Detection theory for graphs. *LINCOLN LABORATORY JOURNAL*, 20(1), 2013.
- [12] Benjamin A Miller, Lauren H Stephens, and Nadya T Bliss. Goodness-of-fit statistics for anomaly detection in chung-lu random graphs. In *Acoustics, Speech and Signal Processing (ICASSP), 2012 IEEE International Conference on*, pages 3265–3268. IEEE, 2012.
- [13] Sebastian Moreno and Jennifer Neville. Network hy-
pothesis testing using mixed kronecker product graph models. In *Data Mining (ICDM), 2013 IEEE 13th International Conference on*, pages 1163–1168. IEEE, 2013.
- [14] Venu Satuluri and Srinivasan Parthasarathy. Scalable graph clustering using stochastic flows: applications to community discovery. In *Proceedings of the 15th ACM SIGKDD international conference on Knowledge discovery and data mining*, pages 737–746. ACM, 2009.
- [15] C Seshadhri, Tamara G Kolda, and Ali Pinar. Community structure and scale-free collections of erdős-rényi graphs. *Physical Review E*, 85(5):056109, 2012.
- [16] Stijn Marinus Van Dongen. Graph clustering by flow simulation. 2000.
- [17] Pak Chung Wong, Harlan Foote, Patrick Mackey, George Chin, Heidi Sofia, and Jim Thomas. A dynamic multiscale magnifying tool for exploring large sparse graphs. *Information Visualization*, 7(2):105–117, 2008.